PERFORMANCE OF THREE-DIMENSIONAL 180°-CURVED DIFFUSER

آداء ناشر منحنى بزاوية ١٨٠ درجة ثلاثي الأبعاد

H. Mansour[a], M. Safwat Mohamed[a], Berge Djebedjian[a] and Sherif A. Yousry[b]

[a] Mechanical Power Engineering Department, Faculty of Engineering, Mansoura University, El-Mansoura 35516, Egypt
E-mails: mhsaadanyh@yahoo.com, msafwat@mans.edu.eg, bergedje@mans.edu.eg
[b] M.Sc. Student, E-mail: sherif.yousry@hotmail.com

الخلاصة:

فى هذا البحث تمت دراسة خصائص السريان فى الناشر المنحنى ١٨٠ درجة ذو نسبة مساحة (٢) ونسبة واجهة (طول إلى عرض) (٢) بإستخدام المجس ذو الخمسة ثقوب. وقد تم معايرة المجس بواسطة جهاز توجيه خاص لعمل ملف بيانات المعايرة والذي يقوم برنامج Multi-probe باستخدامه فى استخراج القياسات المطلوبة. وقد تم قياس المركبات الثلاثة للسرعة والضغط الكلى والاستاتيكي عند مدخل الناشر المنحنى وستة مقاطع عند كل ٣٠ درجة فى إتجاه المخرج، وذلك من الجدار الداخلى للخارجى ومن الجدار العلوى للسفلى. كما تم قياس الضغط الجدارى الاستاتيكى في منتصف المسافة بين الجدارين العلوى والسفلى عند الجدارين الداخلى والخارجى. وقد أظهرت قياسات المركبة الثالثة للسرعة الحركات الفرعية بوضوح، والتى تنتج عن حركة المائع من الجدار الداخلى للخارجى والعكس. وأن المركبة الثانية للسرعة بلغت ٢٠% من سرعة الدخول كحد أقصى نتيجة صغر نسبة الواجهة. بينما بلغت النسبة الكلية لاسترداد الضغط 25.6% من الضغط الديناميكى الداخل نتيجة الحركة الدورانية. وقد أظهرت المقارنة مع نتائج النماذج العددية وجود اختلاف حيث تنبأت هذه النماذج ببدء منطقة الحركة الدورانية متأخرة عن ما أظهرته هذه القياسات. كما أظهرت القياسات نمو الطبقة الجدارية بشكل ملحوظ بينما لم تظهره النماذج العددية.

ABSTRACT

Flow characteristics in $AR = 2$, $AS = 2$, 180° curved diffuser is investigated experimentally by a 5-hole Pitot tube. The Pitot tube is calibrated by a special orientation mechanism to get a calibration data file to be processed by the multi-probe program. Measurements of the three velocity components (u, v, w), total and static pressures for the inlet and six downstream sections located at 30° intervals from the diffuser inlet, from convex to concave walls and top to bottom walls. The wall static pressures in the mid-span between the top and bottom walls at convex and concave walls were measured. Contours of the third velocity component show the secondary motion clearly induced by the movement of fluid from convex to concave wall and reverse. The maximum transverse velocity is about 20% of inlet mean velocity as a result of low aspect ratio of the diffuser exit. The overall pressure recovery achieved was 25.6% of the inlet dynamic pressure due to separation and recirculation occurred at the convex wall. These measurements can be used for the validation and improvement of the turbulence models that used to simulate the flow inside the curved diffuser. It was found that the models predict a later

Accepted September 30, 2010.

NOMENCLATURE

AR	area ratio, W_2/W_1
AS	aspect ratio, H/W_1
C_p	static pressure recovery coefficient
C_{pw}	wall static pressure recovery coefficient
d	hole diameter of five-hole pressure probe, (m)
D	spherical diameter of five-hole pressure probe, (m)
D_h	hydraulic diameter, [$2\ W_1H\ /\ (W_1+H)$], (m)
H	depth of the diffuser, (m)
L	centerline length of the curved diffuser, $L = \pi R_c$, (m)
$L_{1\text{-}9}$	section measuring levels
L_p	length of five-hole pressure probe, (m)
P_{st}	average static pressure along the section, (Pa)
P_{sti}	average static pressure at the inlet, (Pa)
p_w	wall static pressure at a downstream section, (Pa)
p_{wi}	wall static pressure at the inlet, (Pa)
R_c	radius of the diffuser centerline, (m)
Re	Reynolds number, $\rho U_o H/\mu$
U_o	average inlet velocity, (m/s)
u,v,w	Cartesian velocity components
W	width of measured section, (m)
W_1	width of diffuser at inlet, (m)
W_2	width of diffuser at exit, (m)
X	transverse distance measured from convex to concave wall, (m)
y	distance measured from bottom to top wall, (m)

Greek Letters

α	pitch angle
α_{eff}	effective divergence angle, [$AR = 1+ 2(L/W_1)\tan\alpha_{eff}$], (deg)
β	yaw angle, (deg)
δ	cone angle, (deg)
ϕ	roll angle, (deg)
θ	angle of turn, (deg)
ρ	density of fluid, (kg/m^3)

1. INTRODUCTION

In many engineering applications diffusers are used to convert kinetic energy into pressure energy. The importance of the diffuser as a single, useful, fluid-mechanical element in wind tunnels and turbo-machinery has been widely known. Often the flow passages are curved because of space limitations or the arrangement of other components. Flow in curved diffusers is characterized by the presence of vortices or secondary motion due to curvature effects including the imbalance between radial pressure gradient and centrifugal forces. The objectives in curved diffuser study are the determination of pressure recovery; losses and uniformity of flow at exit. While these performance characteristics can be obtained directly from experiments, recently because of the great enhancement in computer capabilities these can be determined computationally using the flow prediction models. However in the development / validation of these models detailed flow data is required, thus, recent experimental studies have therefore tended to focus on the curved diffuser to obtain high-quality data and establish the flow structure.

Fox and Kline [1] indicated the flow dependence on area ratio, inlet aspect ratio, centerline to inlet width ratio, Reynolds number, inlet turbulence intensity and bending angle. They associated that the main problem was the prevention of separation.

McMillan [2] provided high-quality measurements of the mean flow quantities for low speed turbulent flow in 40° turn, $L/W_1 = 3$, $AR = 1.32$, $AS = 1.5$ curved diffuser. He observed two counter-rotating vertical secondary motions between the parallel walls, which dominated the flow behavior.

Rojas et al. [3] generated extensive data on S- and C-shaped curved diffusers having an area ratio of 1.5 and rectangular cross-section. They measured the three components of velocity, wall pressure distribution and UV cross-correlation (for

the turbulent case) along with the pressure recovery.

Shimizu et al. [4] found that energy efficiency can be raised by selecting the correct inlet velocity distribution and generating separation –suppressing-type secondary flow inside the U-bend diffuser.

Majumdar et al. [5] observed the turbulent flow in a high aspect ratio small area ratio 90° curved diffuser using 3-hole pressure probe. They found that no flow reversal except for a very small zone near the exit and the wall static pressure increased continuously on both convex and concave walls. They observed that secondary flows were not strong and counter rotating vortices were observed from 30 degree turn of the diffuser. They indicated that the flow was three dimensional starting from the initial one-third of diffuser length.

Yaras [6] described the inlet boundary layer thickness and turbulence intensity effects on the three components of velocity, static pressure, total pressure distributions, vortices structure and secondary flow in a large-scale 90° curved diffuser.

Majumdar et al. [7] studied the flow structure in 180° bend diffusing duct. They showed the formation of vortex motions and the flow was also seen to shift towards the outer wall exit plane.

Djebedjian [8] predicted a later separation position than experiment by comparing the experimental results of $AS = 2$, $AR = 2$, 180° curved diffuser with numerical results. He used the time-averaged Navier-Stokes equations and the standard and non-equilibrium k-ϵ turbulence models. He achieved an improvement by modifying the constant C_ϵ but the location of the separation point was not displaced.

Mohamed [9] investigated experimentally and numerically the flow in a two-dimensional 180° curved diffuser with a guide vane interposed in the diffuser in various positions. He compared between the measurements in the case of the curved diffuser with and without guide vane. He showed that the presence of a guide vane makes the velocity distribution more uniform and suppresses the region of flow separation. He indicated that the best position for the guide vane was towards the convex wall at $B/W_1 = 0.25$ to 0.333, where B is the transverse distance measured from convex to concave wall.

Djebedjian et al. [10] predicted the mean features of the 2D and 3D turbulent flow in the curved diffuser using numerical turbulent models. They compared the 2D results with the experimental results of Djebedjian [8]. They found that the numerical models predicted later separation position than the experiment. They predicted more reliable results at separation zone by advanced turbulent models. However the main problem is to improve the efficiency and the uniformity of flow inside the diffuser.

Chong et al. [11] improved the uniformity of the flow in a highly unstable 90° curved diffuser by employing several passive flow control devices such as vortex generators, woven wire mesh screens, honeycombs, and guide vanes to control the three-dimensional diffusing flow distribution inside the curved diffuser and hence the exit flow.

In this study, the 180° curved diffuser of **Djebedjian [8]** is used to investigate the flow inside it. A 5-hole Pitot tube is used for measuring the three velocity components (u, v, w), total and static pressure at the inlet and six downstream measuring sections located at 30° intervals from the diffuser inlet. Also, the wall static pressure in the mid-span between the parallel walls at convex and concave walls is measured. These results were compared with the numerical predictions of turbulence models by **Djebedjian et al. [10]** in order to improve the capabilities of these models which give much more facilities in studying alternative designs.

2. EXPERIMENTAL SETUP

The schematic layout of the experimental set-up is shown in Fig. 1. A low turbulence open-type wind tunnel having a cent-axial fan is used in the experiments. The wind tunnel has a variable frequency controller for the motor and a remote speed control device to control the air speed at the bend diffuser inlet using a pre-calibrated curve. The entrance portion is followed by the settling chamber with honeycomb and graduated screens. These reduce the free-stream turbulence to less than 0.5 % at air velocity of 62 m/s. The area ratio of the contraction is 12.5 to 1.0. Constant area straight ducts of lengths 0.3 m and 0.6 m are attached at the diffuser inlet and exit, respectively, to get uni-directional flow at the inlet and the exit. These lengths are 2 times the corresponding diffuser width.

2.1 Test Diffuser

The test diffuser is made from galvanized sheet. It consists of two curved side walls (convex and concave) and parallel top and bottom walls. It has an area ratio AR = 2.0 and circular centerline. The inlet width W_1 is 0.15 m and the inlet height H is 0.3 m, giving an aspect ratio AS of 2. The radius of curvature of the diffuser centerline R_c is 0.3 m and its length L is 0.94 m. Therefore, the radius ratio R_c/D_h is 1.5 and length ratio L/W_1 is 6.27. The effective total divergence angle, 2 α_{eff}, is 9.12 deg. The details of the test diffuser and location of the measuring sections are shown in Fig. 2. The inlet flow conditions to the diffuser are measured in the straight duct at 4 cm upstream of the diffuser inlet. The mass averaged inlet velocity U_o is 33.7 m/s. The Reynolds number based on the inlet hydraulic diameter of the diffuser is 4.59×10^5. The six downstream measuring sections are located at 30 deg intervals from the bend diffuser inlet. Seven static pressure taps exist on each of the curved walls. Seven slots are shaped at the top wall of the test diffuser. Each slot has a width slightly larger than the diameter of the probe holder and extends from the convex to concave walls. The horizontal distance between the probe head and its stem is taken into consideration during the experiments. Therefore, the slots are made parallel to the measuring sections in the downstream direction.

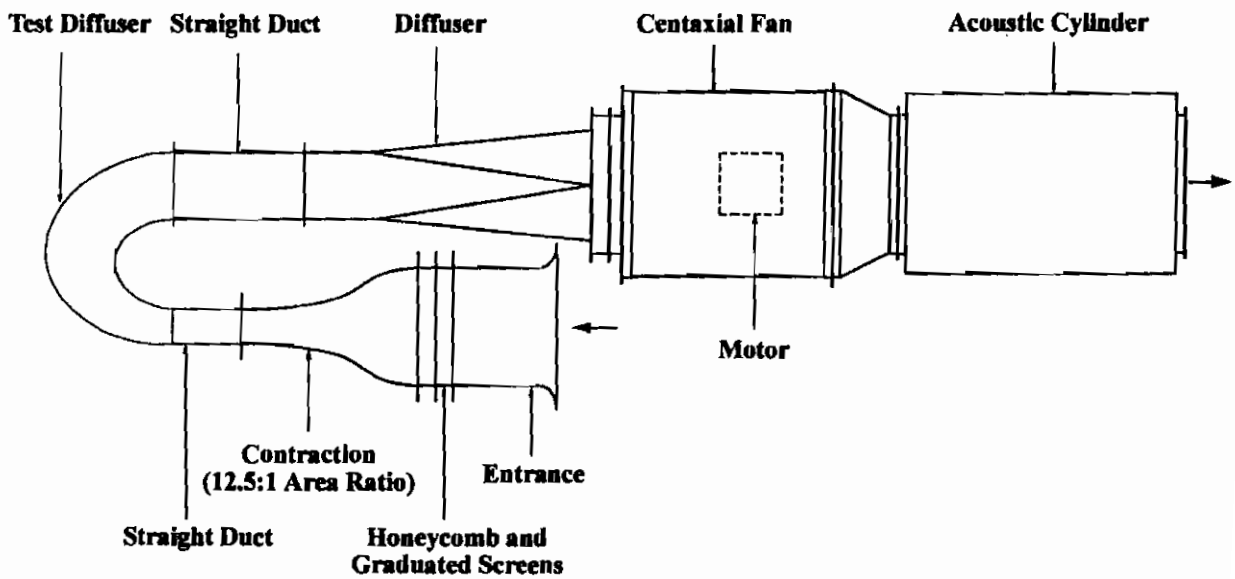

Fig. 1 Experimental setup

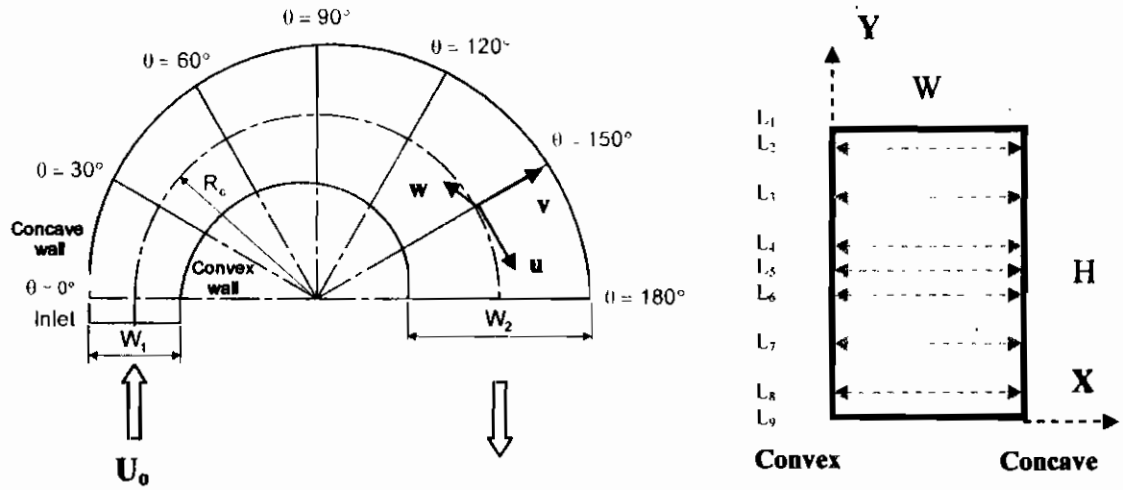

Fig. 2 Diffuser geometry and measuring sections and levels

2.2 Measuring Equipments

2.2.1 Traversing Unit

The calibrated five-hole probe is fixed on a traversing unit that is put above each slot and the probe holder is accommodated in it. It has two axes traversing mechanism and employed to position and report the location of the probe via two precision potentiometers secured to the drive screws. The voltage signal from each potentiometer is transmitted to the digital display in a cabinet meter. The probe traverse mechanism traverses the probe in steps of 2.25 mm. The error in measuring the transverse distance is ± 0.1 mm.

2.2.2 Five-Hole Probe

A five-hole pressure probe, Fig. 3, is used for the measurements of the mean velocities, static and total pressures by the fixed direction method. Its dimensions are: spherical diameter $D = 6$ mm, length $L_p =$ 40 mm, and hole diameter $d = 0.25$ mm.

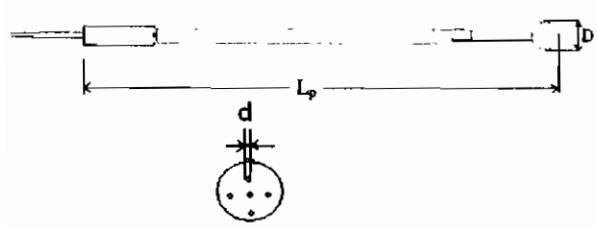

Fig. 3 Spherical straight five-hole pressure probe

2.2.3 Digital Micro-Manometer

The wall static pressures and the pressures sensed by the 5-hole probe are read on a digital micro-manometer. The error in measurement of pressure is ±1%. The blockage created by sensing head of the probe at any measuring point was very small. The measuring circuit was made by connecting the ports of the 5-hole probe to the digital pressure gauge by flexible tubes and ensured that there was no leakage in the circuit.

3. CALIBRATION AND MEASUREMENTS

Multi-Probe program [12] is a data reduction program for 5-hole pressure probes. It can reduce data from probes in any subsonic flow and predict the flow velocity, both direction and magnitude with a high degree of accuracy. It performs two major functions, processing the calibration data for a 5-hole probe and uses this data to find the angles and velocities from port pressures when the probe is in an unknown flow field. It uses at least one calibration file (raw data file) that contains angles and port pressures from the probe during its calibration. This file is converted (preprocessed) to a data file with a standard format. This file can be used to reduce probe data which contains the port

θ = 150° and at diffuser exit. Secondary motion is observed clearly in w contours as a result of vortices and movement of fluid from convex to concave wall and vise versa.

5.2 Pressure

Static and total pressures are normalized by the inlet dynamic pressure ($0.5\rho U_o^2$).

Figure 10 shows the distribution of normalized static pressure contours at the diffuser inlet and the six downstream sections. It is observed to be nearly uniform at the first three sections ($\theta = 0°$, $\theta = 30°$, $\theta = 60°$) especially at far locations from convex wall, the values increase in the direction of concave wall. At $\theta = 90°$ two small pressure nodes appear near the convex wall which increase at $\theta = 120°$ and form a pair of vortices that occupy the whole section at $\theta = 150°$ and disappear at the exit.

Figure 11 shows the distribution of normalized total pressure contours. At the first three sections ($\theta = 0°$, $\theta = 30°$, $\theta = 60°$) it is noticed that the total pressure increases rapidly near the convex wall, reaches its maximum value at the center between the curved walls then decreases till the concave wall. The total pressure in the center is higher in comparison to the pressure close to the parallel walls. At $\theta = 90°$and $\theta = 120°$ the pressure increases till it reaches a constant pressure zone that extends to the concave wall. At $\theta = 150°$ two pressure nodes are formed near the convex wall and at $\theta = 180°$ the pressure increases linearly from the convex to the concave wall.

Figures 12 and 13 illustrate the contours of normalized wall static pressure along the concave and convex walls, respectively.

The static pressure along the concave wall, Fig. 12, increases continuously up to $\theta = 90°$, it remains approximately constant up to $\theta = 150°$ and attaining a maximum pressure recovery of 55% of the inlet dynamic pressure. The pressure then decreases till the exit of the diffuser. The pressure in the center is higher in comparison to the pressure close to the parallel walls. This pressure difference would initiate the flow movement from mid-plane towards the parallel walls. The oscillating variation of the contour lines (particularly the contour lines from $\theta = 90°$ to $\theta = 150°$) indicates the generation of vortices like the formation of a vortex at $\theta = 90°$ close the top wall of the diffuser.

The static pressure along the convex wall, Fig. 13, indicates lower wall static pressure within the straight portion at inlet of the diffuser. It can be attributed to the acceleration of flow along this wall due to strong downstream wall curvature. It is seen that the pressure recovery is slower in the first half of the diffuser compared to the second half. Near the exit of the diffuser it is noticed the formation of two pressure nodes, which may be the start of a vortex pair. The wall static pressure recovery on this wall is 60%.

The wall static pressure recovery coefficient $C_{pw} = (p_w - p_{wi}) / (0.5\,\rho\, U_o^2)$ along the mid-span of convex and concave walls is illustrated in Fig. 14, p_w and p_{wi} are the static pressures at a downstream section and at the inlet, respectively. The figure indicates that the pressure recovery on the convex wall is small in the first 30 deg. This is attributed to the strong downstream curvature, which increases the flow acceleration at this part. The wall pressure recovery on the convex wall is 67% whereas on the concave wall it is 44%. Due to the presence of the recirculation zone in the vicinity of the convex wall in the second half of the diffuser, the bulk velocity shifts to the concave wall resulting in a decrease in the pressure recovery there.

Figure 15 shows the overall pressure recovery along the curved diffuser where a 25.6% of the inlet velocity is achieved as a result of separation and recirculation occurred at the convex wall.

6. CONCLUSIONS

Flow through $AR = 2$, $AS = 2$, 180° curved diffuser have been investigated experimentally. The following conclusions can be drawn:

1. The maximum transverse velocity measured is about 20% of inlet mean velocity as a result of low aspect ratio of the curved diffuser.
2. Contours along the convex and concave walls show pressure recovery of 67%, 44% respectively, while overall pressure recovery along the curved diffuser about 25.6% of the inlet velocity is achieved as a result of separation and recirculation occurred at the convex wall.
3. The oscillating pressure contours indicate the formation of vortices motion near the parallel walls, which grow in size and magnitude till the diffuser exit.
4. Values of w are almost negative due to secondary motion from top to bottom wall. Small positive values appear near the convex wall at $\theta = 120°$till the exit as a result of recirculation at this part of the diffuser.
5. Secondary motion is observed clearly in w contours as a result of vortices and movement of fluid from convex to concave wall and reverse.

Results were compared with the numerical predictions of turbulence models at the mid-span between the parallel walls for the inlet and the six downstream sections, the following conclusions can be drawn:

1. Matching of the longitudinal velocity profiles is good at the inlet and the first three sections downstream these sections separation and recirculation observed experimentally earlier causes poor matching while a significant differences between experimental and numerical transversal profiles as a result of secondary motion.
2. All the models predict a later separation and recirculation position than the experiment, such that separation zone is indicated at $\theta = 120°$ experimentally while the numerical models predict the separation at approximately $\theta = 150°$.
3. Cross flow clearly appear in the experimental contours in a form of vortices motion as a result of fluid moving from concave to convex walls and reverse along the top and bottom walls and a recirculation zone near the convex wall was appear.
4. Curvature effect; appears in the experimental contours; make the flow non uniform and the boundary layer growths near the convex wall while numerical results does not predict such thick boundary layer.

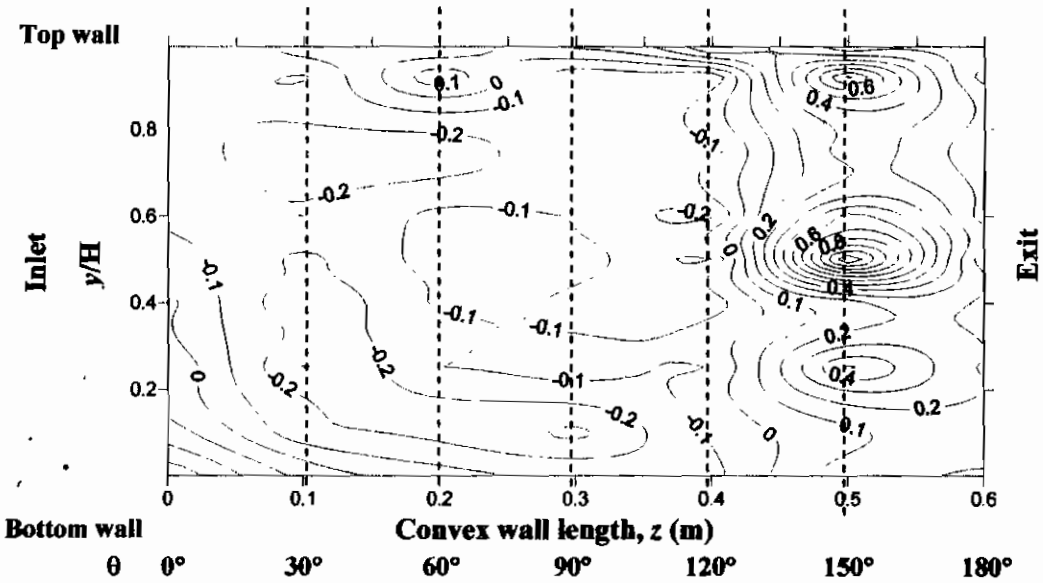

Fig. 13 Normalized convex wall static pressure

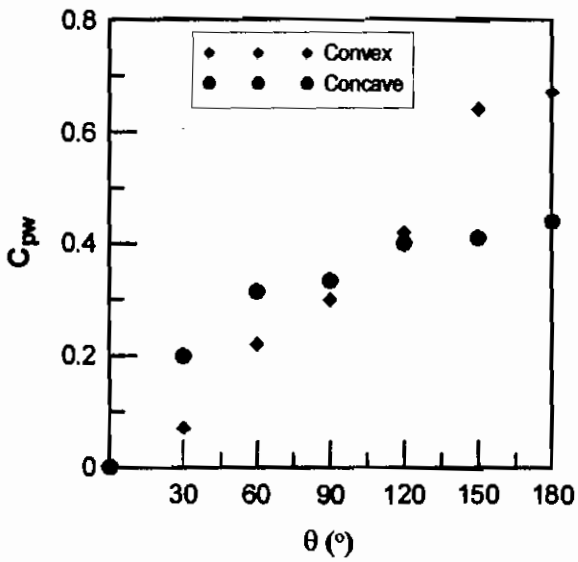

Fig. 14 Variatiou of wall static pressure recovery at convex and concave walls

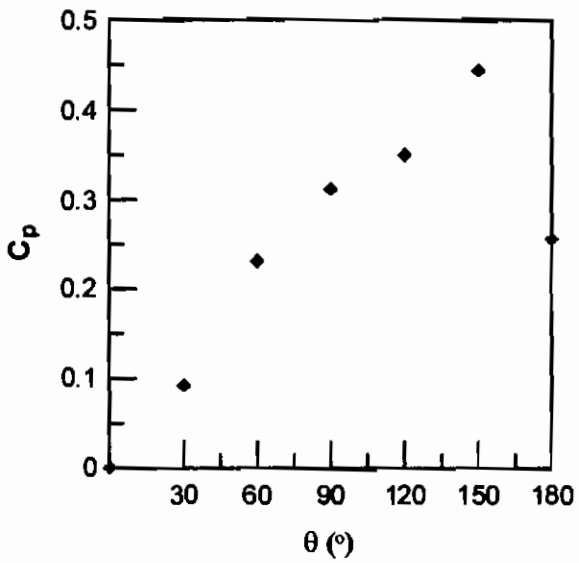

Fig. 15 Variation of the overall static pressure recovery coefficient

References

[1] Fox, R.W., and Kline, S.J., "Flow Regimes in Curved Subsonic Diffusers", *ASME Journal of Basic Engineering*, Series D, Vol. 84, 1974, pp. 303-316.

[2] McMillan, O.J., "Mean-Flow Measurements of Flow Field Diffusing Bend," NASA Contractor Report 3634, 1982.

[3] Rojas, J., Whitelaw, J.H. and Yianneskis, M., "Developing flow in S-Shaped Diffusers," Imperial College of Science & Technology, London (Dept. of Mechanical Engineering) Report No. FS/83/28, 1983.

[4] Shimizu, Y., Nagafusa, M., Sugino, K., and Kubota, T., "Studies on Performance and Internal Flow of U-

Shaped and Snake-Shaped Bend Diffuser," *ASME J. of Fluids Engineering*, Vol. 108, 1986, pp. 297-303.

[5] Majumdar, B., Mohan, R., Singh, S.N., and Agrawal, D.P., "Experimental Study of Flow in a High Aspect Ratio 90 deg Curved Diffuser," *ASME J. of Fluids Engineering*, Vol. 120, 1998, pp. 83-89.

[6] Yaras, M.I., "Flow Measurements in a Fishtail Diffuser with Strong Curvature," *ASME Journal of Fluids Engineering*, Vol. 121, No. 2, 1999, pp. 410-417.

[7] Majumdar, B., Singh, S.N., and Agrawal, D.P., "Flow Structure in 180° Curved Diffusing Duct," *The Arabian Journal for Science and Engineering*, Vol. 24, No. 1B, 1999, pp. 79-87.

[8] Djebedjian, B., "Numerical and Experimental Investigation of Turbulent Flow in a 180-Deg Curved Diffuser," Proceeding of ASME FEDSM' 01, *2001 ASME Fluids Engineering Division Summer Meeting*, New Orleans, May 29-June 1, 2001, Paper No. FEDSM2001-18249.

[9] Mohamed, M.S., "Turbulent Flow in a Two-dimensional 180 Deg Curved Diffuser with Guide Vane," Proceedings of ASME FEDSM'02, *2002 ASME Fluids Engineering Division Summer Meeting*, Montreal, Canada, July 14-18, 2002, Paper No. FEDSM2002-31278.

[10] Djebedjian, B., Mohamed, M.S., and Elsayed, A., "Numerical Investigation of Two- and Three-Dimensional Turbulent Flows in a 180° Curved Diffuser," Proceedings of ICFDP9: *Ninth International Congress of Fluid Dynamics & Propulsion*, December 18-21, 2008, Alexandria, Egypt.

[11] Chong, T.P., Joseph, P.F., and Davies, P.O.A.L., "A Parametric Study of Passive Flow Control for a Short, High Area Ratio 90 Deg Curved Diffuser," *ASME, J. of Fluids Engineering*, Vol. 130, No. 11, 2008, pp. 111104.1-111104.12.

[12] Multi-Probe Program, Aeroprobe Corporation designed by Espen S. Jansen, NASA Langley Research Center, http://www.aeroprobe.com

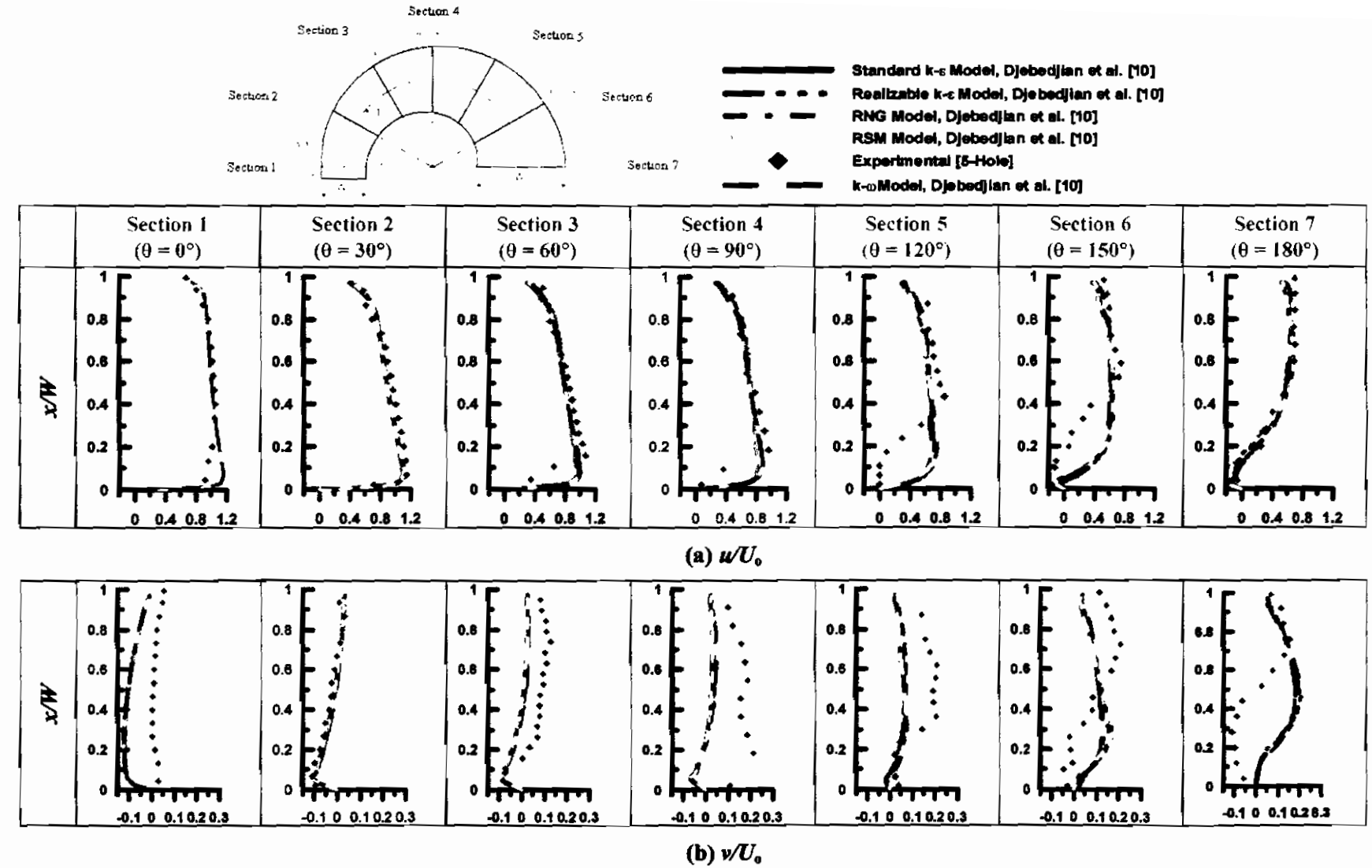

(a) u/U_o

(b) v/U_o

Fig. 5 Comparisons of experimental and numerical longitudinal (u) and transversal (v) velocity components at $y/H = 0.5$

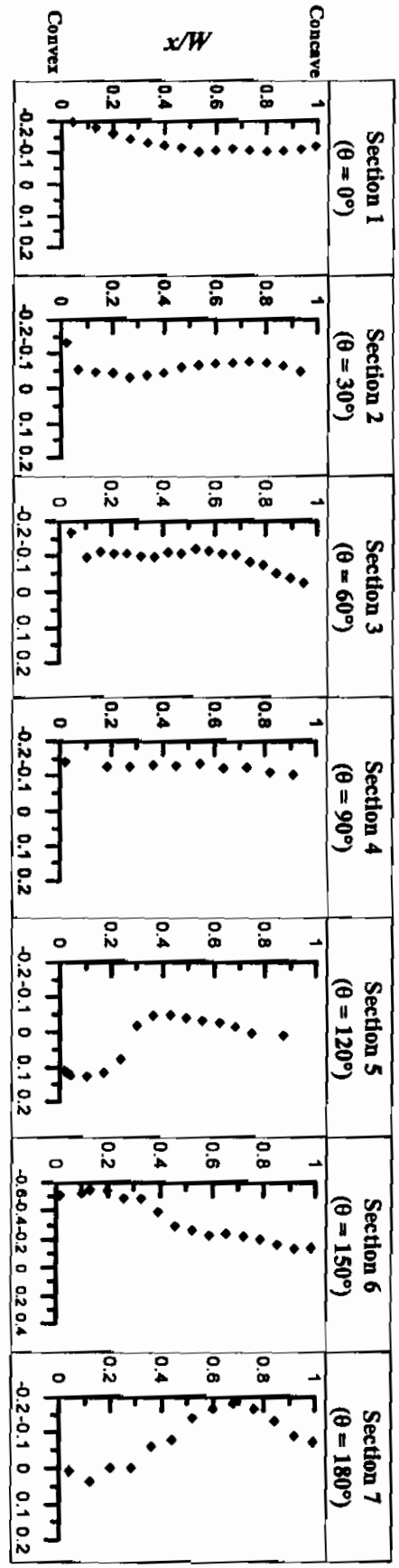

Fig. 6 *w* profiles at inlet and the six downstream sections

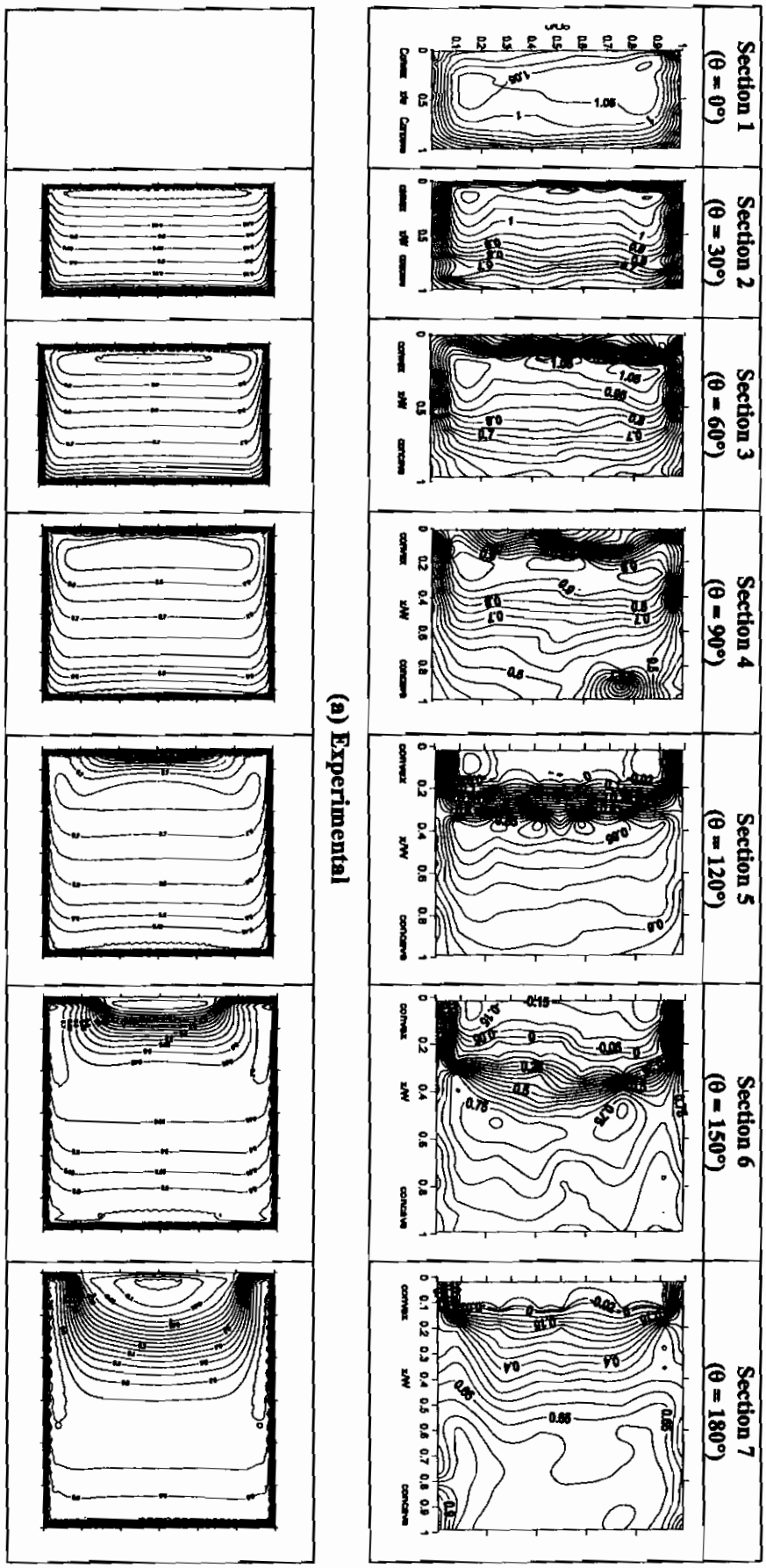

Fig. 7 Comparison between present experimental and numerical results of Djebedjian et al. [10] for the longitudinal velocity contours

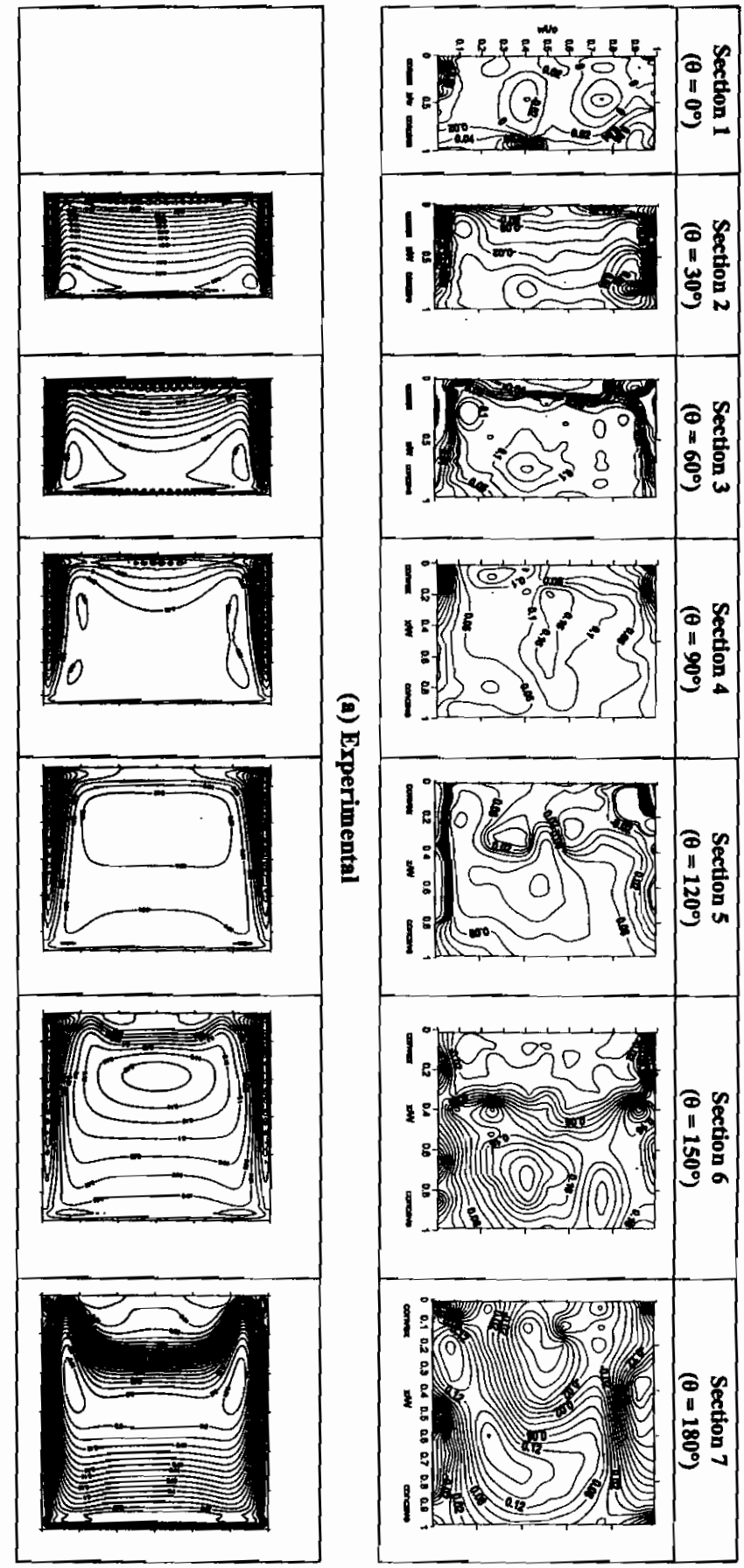

Fig. 8 Comparison between present experimental and numerical results of Djebedjian et al. [10] for the transversal velocity contours

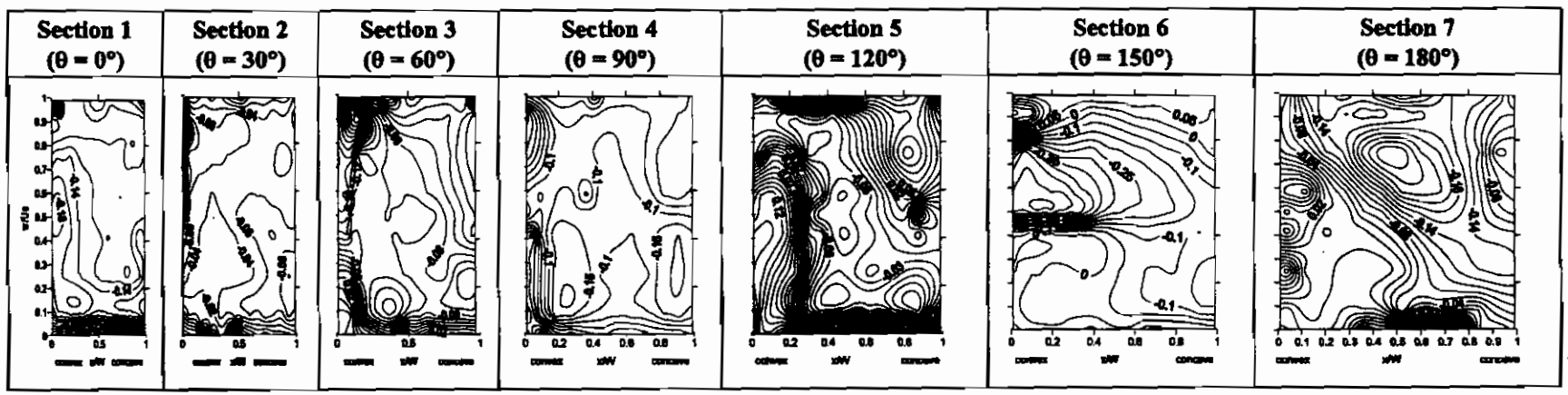

Fig. 9 Contours of *w* velocity component

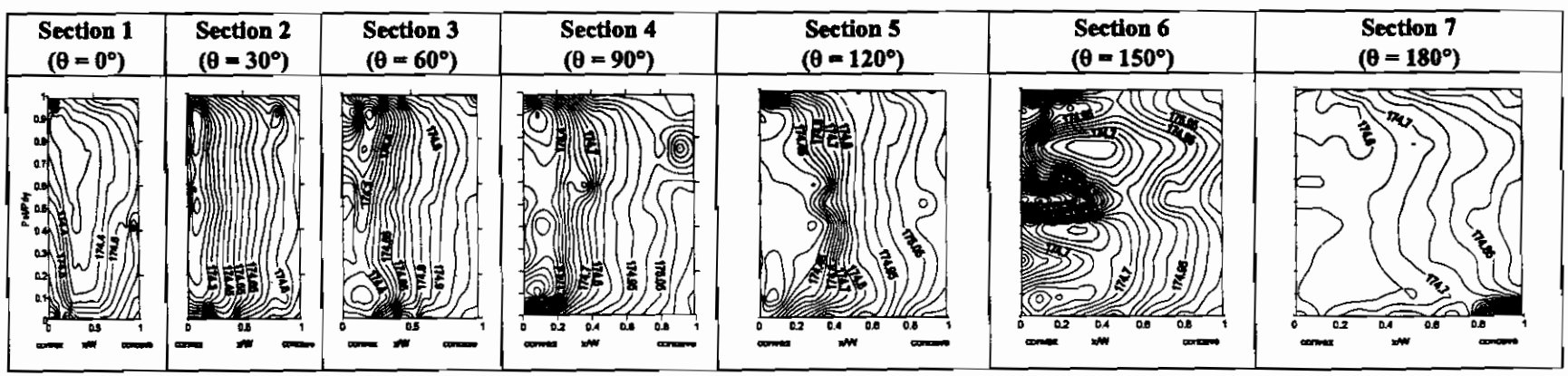

Fig. 10 Normalized static pressure contours

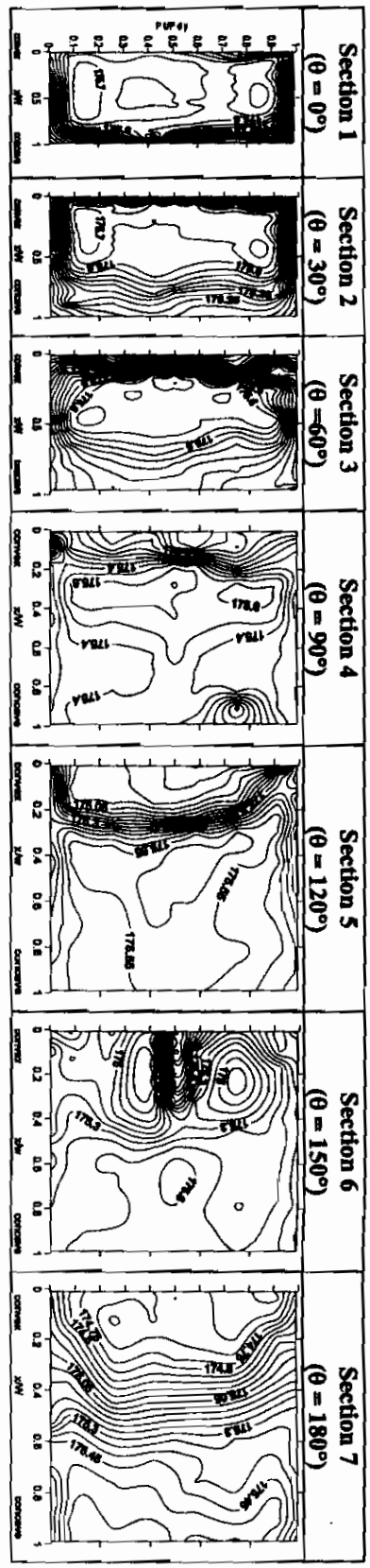

Fig. 11 Normalized total pressure contours

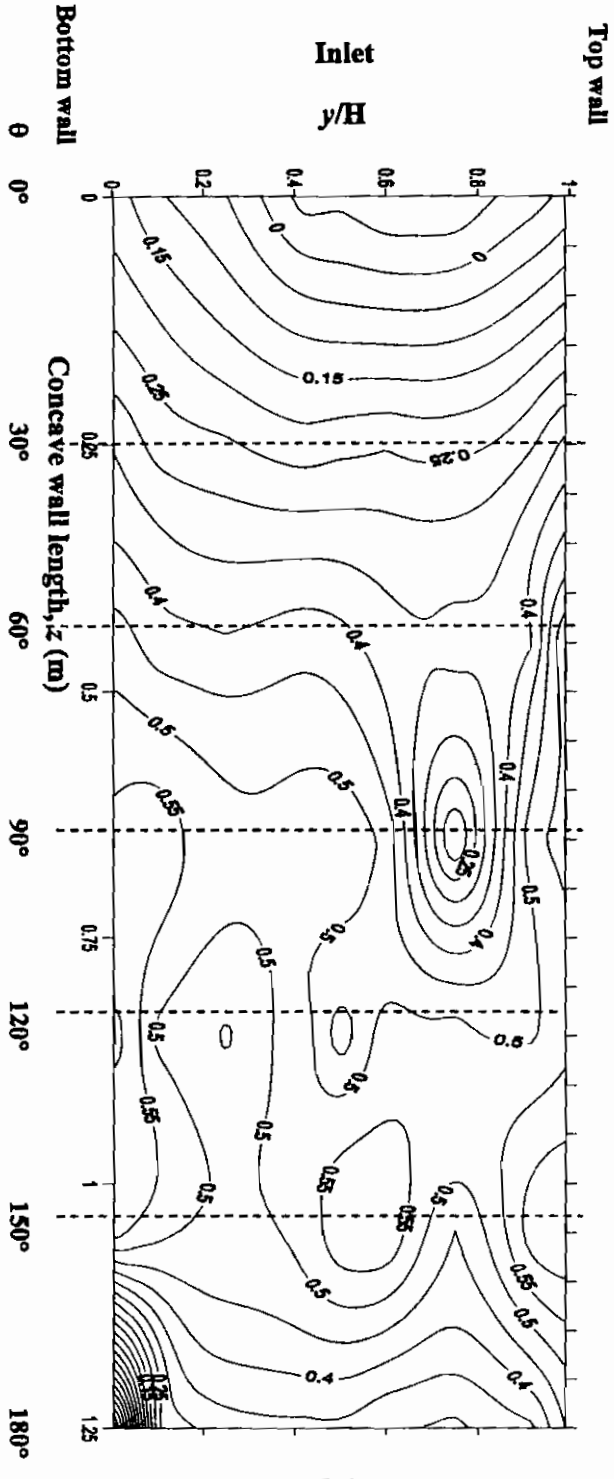

Fig. 12 Normalized concave wall static pressure